Density-functional calculation of multiple-shock Hugoniots of liquid nitrogen

S. Mazevet, J. D. Johnson, J. D. Kress, and L. A. Collins
Theoretical Division, Los Alamos National Laboratory, Los Alamos, New Mexico 87545

P. Blottiau
CEA, BP12 F91680, Bruyères Le Châtel, France
(Received 21 May 2001; published 12 December 2001)

We have performed molecular dynamics simulations at fixed density and temperature points to obtain the internal energy and pressure of shock-compressed fluid nitrogen. Our calculations were performed using the generalized gradient approximation in density functional theory. While the single-shock Hugoniot derived from this equation of state agrees well with gas-gun experiments, in contrast, the second-shock Hugoniots show discrepancies with the experimental measurements. This is particularly the case in the region where negative Grüneisen parameters were deduced experimentally and where shock cooling was measured.

DOI: 10.1103/PhysRevB.65.014204 PACS number(s): 71.15.Pd, 62.50.+p, 61.20.Ja

I. INTRODUCTION

Given its ability to form numerous chemical counpounds, nitrogen has considerable impact on a wide variety of fields[1] embracing fluids, geology, shocks, detonation, and biology. A particularly fertile area of investigation is the study of fluid nitrogen under compression, specifically the equation of state (EOS). Experiments[2–5] have indicated that the first- and second-shock Hugoniots exhibit the following characteristic features: a softening of the principal Hugoniot as the density increases, negative values of the Grüneisen parameter, and shock-induced cooling when the material is reshocked. Physically, a negative value of the Gruneisen parameter implies a negative thermal expansion which, in some cases, may indicate a phase transition. We generally associate heating with the passage of a shock through a medium so that the possible cooling presages an additional energy sink. All these effects have been attributed to the dissociation of molecular nitrogen as the increasing compression and temperature break the molecular bond.

We have recently demonstrated that *ab initio* molecular dynamics (MD) provides a sound description of the EOS of fluid nitrogen along the principal Hugoniot,[6] based on agreement with various gas-gun experiments. We now turn to the description of multiple-shock Hugoniots and shock-induced cooling. The latter is a very unusual feature, which was observed experimentally by Nellis and co-workers.[3,4] Shock-induced cooling can occur when, at the higher pressure and densities of the second shock, the dissociation of molecular nitrogen absorbs a sufficient amount of energy that the temperature of the medium actually decreases from that of the initial shock state.[4] The mechanism involved has been subsequently investigated using various models based on integral equation and fluid perturbation theory.[7–12] Yet, due to the parametric nature of such approaches, the general understanding such models provide of the experimental data seems questionable without further *ab initio* calculations or experimental support. To our knowledge, the experimentally observed shock-induced cooling for liquid nitrogen has never been investigated using *ab initio* methods. In this study, we present a multiple-shock Hugoniot produced using a finite-temperature density-functional theory (DFT) at the generalized gradient approximation (GGA) level.

II. COMPUTATIONAL METHOD

Over the past few years, a variety of large-scale simulation methods have been developed to treat fluid systems over a broad range of conditions. Among the most sophisticated approaches one finds the path-integral Monte Carlo [13] (PIMC) and density-functional molecular dynamics[14–16] (DFT-MD) methods. In finite-temperature DFT approaches (FTDFT-MD) as used in the present work,[14,16] the total energy is written as a functional of the electron density, which is obtained by summing the probability density over occupied electron orbitals, populated according to a Fermi-Dirac distribution at temperature T_e. Further, for GGA formulations, electronic exchange and correlation energy are approximated using a functional which depends only on the electron density and its spatial derivatives. GGA methods provide a highly accurate means of studying the thermochemistry of chemical bonding by representing the inhomogeneities inherent in the electron charge density. In addition, the method encompasses all manner of transient effects such as dissociation and association of chemical bonds, quasimolecular formation, ionization, and recombination. We employed the VASP plane-wave pseudopotential code, which was developed at the Technical University of Vienna.[17] This code implements the Vanderbilt ultrasoft pseudopotential scheme[18] in a form supplied by Kresse and Hafner[19] and the Perdew-Wang 91 parametrization of the GGA.[20]

We performed fixed-volume molecular dynamics simulations at separate density and temperature points, selected to span a range of densities from $\rho = 1.50$ to 2.9 g/cm^3 and temperatures from $T = 1000$ to 20000 K that highlight the second-shock Hugoniot region. We used 32 and 64 nitrogen atoms in the unit cell and fixed the plane-wave cutoff at 435 eV. Integration of the equations of motion proceeded with time steps of 2 fs. Typical simulations ran for 400 time steps with the initial condition derived from a configuration at the same density and lower temperature. We typically let the system equilibrate for 100 time steps and then calculated

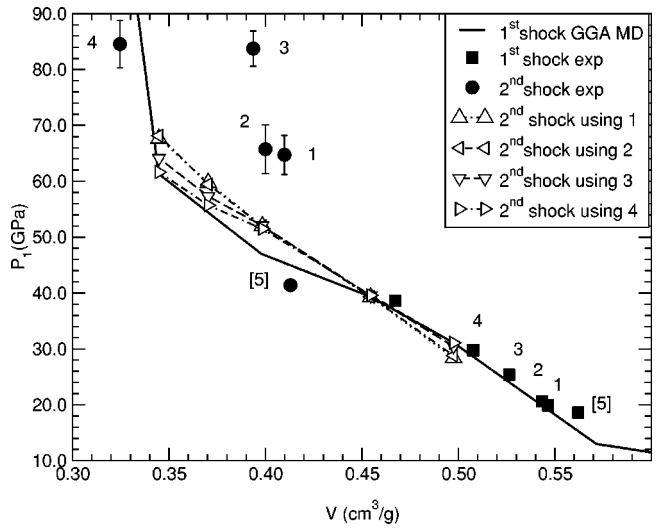

FIG. 1. Comparison between the experimental data of Ref. 4 (points 1–4) and Ref. 5 (point 5) and GGA-MD nitrogen first- and second-shock Hugoniots.

properties using the final 300 time steps. This procedure proved sufficient to obtain accurate thermodynamic quantities, including pressure and internal energy, when compared to calculations with longer trajectory times of up to 900 time steps for 64 atoms. The statistical error in the thermodynamical quantities—pressure and internal energy—reported in this work is of the order of 10% or less. We employ both microcanonical and isokinetic ensembles for the ions. In the latter, the ion temperature T_i is fixed using velocity scaling. In turn, the assumption of local thermodynamic equilibrium sets the electron temperature T_e to that of the ions T_i. In the region of interest to the present study, both ensembles give consistent thermodynamical properties (i.e., pressure and internal energy).

The principal and multiple-shock Hugoniots satisfy the Rankine-Hugoniot equation

$$(U_0-U_1)+\frac{1}{2}(V_0-V_1)(P_0+P_1)=0, \qquad (1)$$

where 0 and 1 refer, respectively, to the initial and final conditions. U is the internal energy, V the volume, and P the pressure. The shock Hugoniot points (P_1, T_1) are determined by solving Eq. (1) using a least-squares fit to a quadratic function in T of P and U. Specific details of the procedure used to calculate the Hugoniot points can be found in Ref. 6.

III. RESULTS AND DISCUSSION

A. Second-shock Hugoniots

Figure 1 shows the calculated and measured first- and second-shock Hugoniot points. For the experimental points, the numerical labels displayed on the figure associate the first Hugoniot points to the resulting second-shock Hugoniot points when the former are reshocked. The first-shock Hugoniot points are obtained by impacting cryogenic liquid nitrogen initially at a density of $\rho_0=0.808$ g/cm^3 ($V_0=1.237$ cm^3/g) and a temperature of $T_0=77$ K. Due to the good agreement between the first-shock GGA-MD Hugoniot[6] and the experimental measurements in this density region, we used the experimental first-shock data of Nellis *et al.*[4] as initial conditions to calculate the second-shock Hugoniots. As can be noticed from Eq. (1), each of the experimental second-shock points, corresponding to a particular initial state, belong to different second-shock Hugoniots. As the experimental data indicate a strong sensitivity to the initial and final states, we used, for each of the four initial experimental conditions, several of our fixed density and temperature simulations to generate the second-shock Hugoniots over a region which spans densities from $\rho=2$ g/cm^3 ($V=0.5$ cm^3/g) to $\rho=2.9$ g/cm^3 ($V=0.3448$ cm^3/g).

As seen in Fig. 1, significant disagreement exists between the predicted and measured second-shock Hugoniot points around $\rho=2.5$ g/cm^3 ($V=0.4$ cm^3/g). Experimental measurements indicate second-shock pressures much higher than those of the first-shock Hugoniot when compared at fixed density. On the other hand, the GGA-MD simulations using 32 atoms show second-shock Hugoniot points only slightly above the first-shock values in this region. The theoretical second-shock Hugoniot points have a lower pressure than the first-shock ones at the smallest density $\rho=2.0$ g/cm^3 ($V=0.5$ cm^3/g) and move above the first-shock Hugoniot between $\rho=2.2$ g/cm^3 ($V=0.454$ cm^3/g) and $\rho=2.9$ g/cm^3 ($V=0.344$ cm^3/g) where they cross again the principal Hugoniot. Further, while the general trend of the experimental second-shock Hugoniot points is reproduced by the GGA-MD predictions, the latter do not show the sensitivities to the initial conditions suggested by the measurements. The experimental measurements suggest that a variation of the first-shock density from 1.84 g/cm^3 ($V=0.5434$ cm^3/g) to 1.9 g/cm^3 ($V=0.5263$ cm^3/g) is reflected in a difference of 20 GPa in the final second-shock pressures (e.g., experimental points 2 and 3 in Fig. 1). This contrasts with the theoretical findings that show that the final second-shock pressures do not differ by more than 5 GPa in this region when the initial conditions are varied accordingly.

At fixed density, the relative positions of the first- and second-shock Hugoniot points have direct implications on the values of the Grüneisen parameter. The Grüneisen parameter is defined as

$$\gamma=V\left(\frac{\partial P}{\partial E}\right)_V=\frac{1}{C_V}\left(\frac{\partial P}{\partial T}\right)_V, \qquad (2)$$

where C_V, the specific heat capacity, is positive for thermodynamic stability. Experimentally, a negative Grüneisen parameter was deduced in this region, an effect attributed to a transition from a molecular to an atomic fluid[3] (sometimes referred to as a ''continuous phase transition''). Physically, a negative value of the Gruneisen parameter implies a negative thermal expansion as well as a decrease in pressure as a function of a positive increase in temperature as seen from Eq. (2).To examine this further in the context of our simulation, it is useful to inspect nitrogen isochors at densities reached by the second shock.

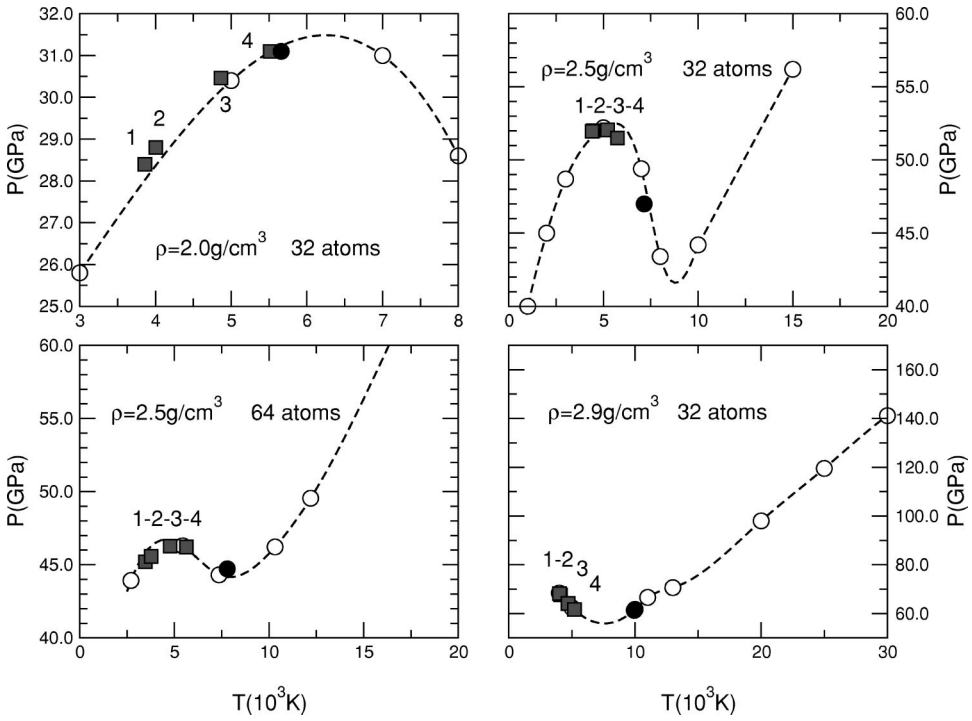

FIG. 2. Comparison of the first- and second-shock Hugoniot points in P/T space at constant densities. GGA-MD simulation (open circle), first-shock Hugoniot points (solid circle), and second-shock Hugoniot points (gray square). The densities and number of atoms are indicated in each graph. Labels 1, 2, 3, and 4 correspond to various initial states as described in the text.

Figure 2 shows the nitrogen isochors for simulations at 3 different densities using a unit cell of 32 atoms and one density using 64. In addition, we also display at each density the position of the theoretical principal and second-shock Hugoniot points on each isochor. The labels of the second-shock Hugoniot points match those of Fig. 1. By taking the finite difference in pressure and temperature for the first- and second-shock Hugoniot points in Fig. 2, we find that the Grüneisen parameter is positive at $\rho=2.0$ g/cm^3, negative at $\rho=2.5$ g/cm^3, and again positive at $\rho=2.9$ g/cm^3. While the calculations indicate that the predicted Grüneisen parameter is negative at a density around $\rho=2.5$ g/cm^3, in accordance with the experimental finding, a significant cell-size dependence is found. As the sample is increased from 32 to 64 atoms, a sizable reduction of the slope of the isochor at $\rho=2.5$ g/cm^3 and around $T=5000$ K is noticeable, mainly affecting the final pressures of the second-shock points. The final pressure of the principal Hugoniot point at this density varies only slightly from $P=47$ to 45 GPa as the cell size is increased. A similar cell-size dependence for the isochors was also observed in GGA-MD simulations of dense hydrogen over the dissociating region.[16] As confirmed by a cluster analysis and comparison of the radial distribution functions obtained between the two simulations, the limited number of atoms (32 relative to 64) used in the unit cell tends to decrease the dissociation fraction in the media for this sensitive density region. For densities around $\rho=2.5$ g/cm^3, the 32-atom simulations should be considered as an upper bound for the absolute value of the Grüneisen parameter. Consequently, the main result of our GGA-MD simulation in the dissociating region indicates that the Grüneisen parameter is near zero, maybe slightly negative, but not as negative as the experimental measurements suggest. Given the sensitivity shown in this density region, the simulations for even more atoms could yield a positive value of the Grüneisen parameter.

It is interesting to go a little further and determine the implications of the above disagreement. We first turn to the question of the character of the reflected second wave. In Ref. 21 it was proposed that the reflected waves in the region of dissociation were not single shocks but instead composite waves consisting of multiple shocks and isentropic compressions. This can be seen in the data displayed in Fig. 1. If a straight line is drawn between the initial and final states labeled 4, this Rayleigh line intersects the reshock Hugoniots for the points 1, 2, and 3 which implies that a single shock for point 4 is unstable[22] and composite waves must be considered. While our simulations do not preclude single second shocks that are stable, they are, to within uncertainties, consistent with a composite-wave picture, and we believe that complex, spreading, reflected waves are very probable. In Ref. 21 it was speculated that a reanalysis of the experimental data (points 1, 2, and 3) in terms of a complex reflected wave would move the plotted final states to the neighborhood of the first-shock (principal) Hugoniot. However, detailed calculations show that the final-state points 1, 2, and 3 are moved only slightly closer to the principal Hugoniot and that the composite-reflected-wave picture does not resolve completely the disagreement shown in Fig. 1. The origin for such a small difference in the reanalysis of the experiment in terms of a composite wave can be traced back to the small value of the Gruneisen parameter in this region. For small values of γ, an adiabat and a shock lead to similar final pressures.

We now consider the experimental measurements of Schott *et al.*[5] These three reflected-wave points all lie below the principal Hugoniot. The second shock for which the

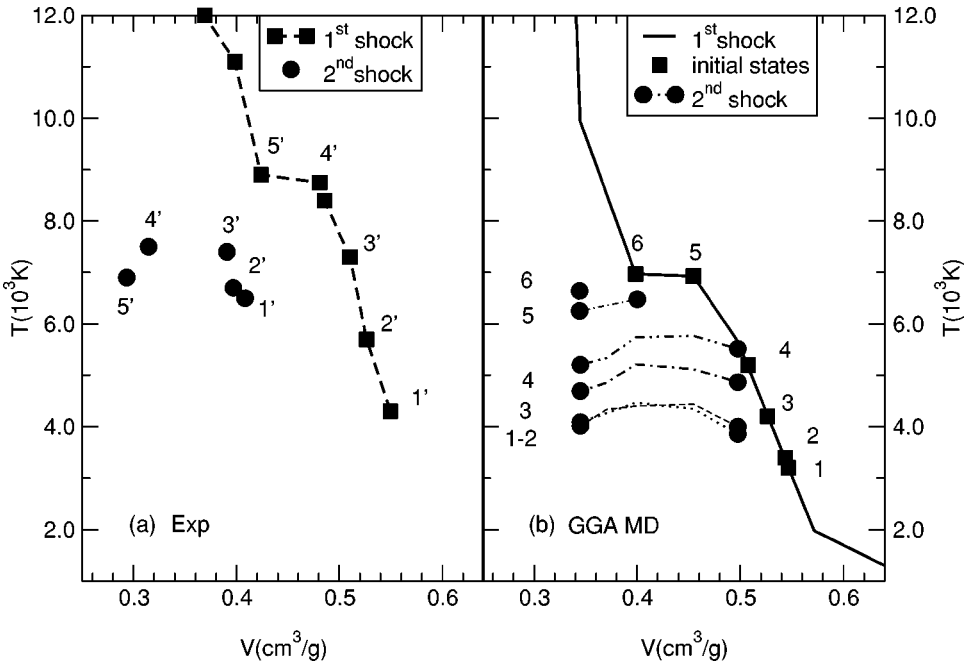

FIG. 3. (a) Measured temperature variation along the first- and second-shock Hugoniots from Ref. 4. (b) GGA-MD results.

highest pressure was reached is shown in Fig. 1 along with the corresponding first-shock point. As can be seen in Fig. 1, the first-shock densities of points 1, 2, and 5 are very close. Consequently, the final pressure for point 5, coupled with points 1, 2, and 3, can be interpreted two ways: a rapidly dropping Grüneisen parameter going strongly negative[3,4] or contradictory data from two different experiments. Second, on the theoretical side, there is a remarkably good agreement between the present *ab initio* approach, the integral equation theory,[7] and even the linear mixing model[8,9] which, despite its flexibility in describing the experimental data, also fails to match the reported second-shock Hugoniot pressures at densities around $\rho=2.5$ g/cm^3. In summary, while it is not the intent of the present study to pass judgement on the different experimental practices used to perform these two sets of measurements, we note that relevant differences in the shock detection techniques might explain this apparent disagreement. In connection with this, we find that only a 3% shift of the measured shock velocities in Ref. 4 results in measured second-shock Hugoniot pressures, in agreement with our simulations.

B. Second-shock temperature and "shock cooling"

We now turn to another characteristic feature of shock-compressed nitrogen: the second-shock temperatures and shock-induced cooling. We show, in Fig. 3, a comparison of the predicted and measured temperatures along the first- and second-shock Hugoniots. In Fig. 3(a), labels $1'$, $2'$, $3'$, $4'$, and $5'$ correspond to initial and final experimental states where temperature measurements were performed using pyrometric techniques.[4] We also note that these experimental points correspond to different shock conditions from those shown in Fig. 1. The calculations in Fig. 3(b) match the experimental first-shock points of Fig. 1 for the points 1–4. The shocks labeled 5 and 6 are calculated using GGA-MD first-shock points. The theoretical temperatures shown in Fig. 3(b) were obtained using 32 atoms in the simulation cell.

First, it should be noted that while the main feature of the temperature variation along the principal Hugoniot is reproduced, a consistent shift to lower temperature is observed in the dissociating region for the simulations.[6] A consistent shift, roughly of the same amount, is also evident for the second-shock temperatures. The experimental measurements suggest second-shock temperatures around 7000 K while the calculations indicate corresponding second-shock temperatures on average around 5500 K. The simulations, however, also share strong similarities with the experimental data. First, along each second-shock Hugoniot, the temperature is almost constant as the density increases. Second, in this particular region, very little variations in temperature between the first- and second-shock points are noticeable, also in accordance with the experimental measurements. For example, the shock labeled $3'$ in Fig. 3(a) indicates that a nearly constant temperature of around 7500 K is measured for the first shock at a density of $\rho=2.0$ g/cm^3 ($V=0.5$ cm^3/g) as well as when the material is reshocked and reaches a density of $\rho=2.5$ g/cm^3 ($V=0.4$ cm^3/g). Figure 3(b) shows that such a feature is reproduced by the calculations. For example, the shock labeled 4 in Fig. 3(b) also indicates that, over this density region, the temperature is almost held constant between the two shocks at around 5000 K.

To further understand the temperature variation between the first and second shocks, it is instructive to consider the constituency of the fluid as given by our simulation at each of the corresponding conditions. In Fig. 4 we show the variation of the dissociation fraction along the principal Hugoniot and the 5000 K isotherm. The dissociation fraction represents the percentage of monomers constituting the fluid relative to the total number of atoms in the simulation cell. The dissociation fraction is obtained by performing a cluster analysis[23] of the MD trajectories. This procedure involves

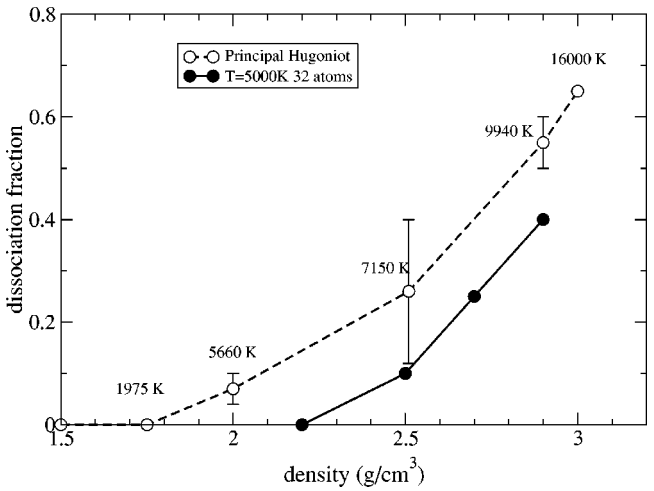

FIG. 4. Comparison of the dissociation fraction along the principal Hugoniot Ref. 6 and the 5000 K isotherm.

selecting an effective radius—in the present case $r_c = 2.3a_B$—and considering all atoms within this distance as bound to a reference atom. The distribution of monomers, dimers, and larger molecules obtained at each time step is subsequently averaged over the whole trajectory. Figure 4 shows that along the first Hugoniot, as the density, pressure, and temperature increase, the initially diatomic fluid continuously dissociates. As seen in Fig. 3, the dissociation of the fluid between a density of 2.0 g/cm^3 ($V = 0.5$ cm^3/g) and 3.0 g/cm^3 ($V = 0.33$ cm^3/g) corresponds to the marked inflection of the principal Hugoniot temperature in this region.[6] Figure 4 also shows that, held at a fixed temperature of 5000 K, the fluid also dissociates continuously as the density is increased from 2.2 g/cm^3 ($V = 0.45$ cm^3/g) to 3.0 g/cm^3 ($V = 0.33$ cm^3/g).

We consider now points 1–4 shown in Fig. 3(b) where the second-shock temperatures are almost constant (around 5000 K in conjunction with variation of the dissociation fraction along the 5000 K isochor displayed in Fig. 4). This comparison clearly suggests that molecular dissociation is also responsible for the weak temperature variation along the second-shock Hugoniot and between the first- and second-shock Hugoniots. For example, the shock labeled 3 on Fig. 3(b) indicates a temperature variation of around 800 K between the first and second shocks when the density reached by the second shock is around 2.2 g/cm^3 ($V = 0.45$ cm^3/g). The corresponding dissociation fractions for the initial and final states shown in Fig. 4 indicate that in this regime the fluid stays undissociated. This suggests that the excess energy is mostly transferred to the fluid as kinetic energy. As the final density of the second shock is increased, the fluid gradually dissociates and the additional excess energy is mostly all absorbed in breaking the molecular bounds. Such an interpretation of the origin of the constant second-shock temperature that we deduced from the results of the GGA-MD simulations is also similar to the one suggested within the linear mixing model.[8]

We finally turn to the measurements where shock cooling was observed (points 4′ and 5′) in Fig. 3(a). To investigate this effect, we calculate second-shock Hugoniot points using GGA-MD first-shock points [points 5 and 6 in Fig. 3(b)] located near the temperature inflection point. The calculations using 32 atoms shown in Fig. 3(b) indicate that a slight cooling of around 500 K might be present when the liquid is shocked with an initial density around 2.5 g/cm^3 ($V = 0.4$ cm^3/g). However, more precise calculations of the first- and second-shock points using 64 atoms in the simulation cell reduce the effect and bring the first- to second-shock temperature variation to near zero and within our estimated uncertainty of the state of the fluid. This contrasts with the experimental measurements which suggest a significant drop in temperature (1000–2000 K). Using the 64-particle simulations for point 6, we further find that an increase of 0.5 eV/atom in the difference between the first- and second-shock internal energies is necessary to obtain agreement with the experimental data and observe a cooling of 1500 K in this region. This estimate is outside of our uncertainties in the first- and second-shock internal energies. To obtain qualitatively the experimentally measured shock cooling, the fluid needs to be either less dissociated in the initial state or more dissociated in the final state, or some combination of both. Overall, given the uncertainties in the experimental measurements as well as in our simulations, we believe that there is still agreement on the general features of the multiple-shock temperature variation.

IV. CONCLUSION

In summary, despite the excellent agreement between the GGA-MD simulation for the experimental principal Hugoniot, we now find noticeable disagreement for the second-shock Hugoniots. Such discrepancies reflect upon the estimated value of the Grüneisen parameter over the dissociating region which we found to be near zero and not as negative as suggested experimentally. This is also the case for measurements where shock cooling was observed. While the simulations suggest that the temperature variation between the first and second shocks can be small and close to zero, we do not find evidence for a large decrease in temperature as suggested by the experimental data. Overall, while there is qualitative agreement between the GGA-MD and the experimental measurements on the behavior of the second-shock nitrogen Hugoniot, the quantitative agreement obtained for the first-shock data no longer pertains for the multiple shocks.

ACKNOWLEDGMENTS

The work at the Los Alamos National Laboratory was supported by the U.S. Department of Energy through Contract No. W-7405-ENG-36. We would like to thank W. Nellis, N. Holmes, R. Chau, and W.W. Wood for many useful discussions.

[1] P. J. Kortbeekm, C. A. T. Seldam, and J. A. Schouten, Mol. Phys. **69**, 1001 (1990); H. D. Jones and F. J. Zerilli, J. Appl. Phys. **69**, 3893 (1991); J. Touret and A. M. van den Kerkhof, Physica (Utrecht) **139**, 834 (1986).
[2] R. D. Dick, J. Chem. Phys. **52**, 6021 (1970).
[3] H. B. Radousky, W. J. Nellis, M. Ross, D. C. Hamilton, and A. C. Mitchell, Phys. Rev. Lett. **57**, 2419 (1986); W. J. Nellis, N. C. Holmes, A. C. Mitchell, and M. van Thiel, *ibid.* **53**, 1661 (1984).
[4] W. J. Nellis, H. B. Radousky, D. C. Hamilton, A. C. Mitchell, N. C. Holmes, K. B. Christianson, and M. van Thiel, J. Chem. Phys. **94**, 2244 (1991).
[5] G. L. Schott, M. S. Shaw, and J. D. Johnson, J. Chem. Phys. **82**, 4264 (1985).
[6] J. D. Kress, S. Mazevet, L. A. Collins, and W. W. Woods, Phys. Rev. B **63**, 024 203 (2001).
[7] M. Ross and F. H. Ree, J. Chem. Phys. **73**, 6146 (1980).
[8] M. Ross, J. Chem. Phys. **86**, 7110 (1987).
[9] M. Ross, High Press. Res. **16**, 371 (2000).
[10] M. van Thiel and F. H. Ree, J. Chem. Phys. **104**, 5019 (1986).
[11] L. E. Fried and W. M. Howard, J. Chem. Phys. **109**, 7338 (1998).
[12] D. C. Hamilton and F. H. Ree, J. Chem. Phys. **90**, 4972 (1989).
[13] B. Militzer and D. Ceperley, physics/0001047 (unpublished); B. Militzer and E. Pollock, Phys. Rev. E **61**, 3470 (2000).
[14] T. Lenosky, S. Bickham, J. Kress, and L. Collins, Phys. Rev. B **61**, 1 (2000).
[15] G. Galli, R. Hood, A. Hazi, and F. Gygi, Phys. Rev. B **61**, 909 (2000).
[16] S. Bagnier, P. Blottiau, and J. Clerouin, Phys. Rev. E **63**, 015 301(R) (2001).
[17] G. Kresse and J. Hafner, Phys. Rev. B **47**, 558 (1993); G. Kresse and J. Furthmüller, Comput. Mater. Sci. **6**, 15-50 (1996); Phys. Rev. B **54**, 11 169 (1996).
[18] D. Vanderbilt, Phys. Rev. B **41**, 7892 (1990).
[19] G. Kresse and J. Hafner, J. Phys.: Condens. Matter **6**, 8245 (1994).
[20] J. P. Perdew, in *Electronic Structure of Solids*, edited by F. Ziesche and H. Eschrig (Akademie Verlag, Berlin, 1991).
[21] J. D. Johnson, High Press. Res. **16**, 305 (2000); Phys. Rev. E **59**, 3727 (1999).
[22] R. Menikoff and B. J. Plohr, Rev. Mod. Phys. **61**, 75 (1989).
[23] T. J. Lenosky, J. D. Kress, L. A. Collins, and I. Kwon, Phys. Rev. B **55**, R11 907 (1997); T. J. Lenosky, J. D. Kress, and L. A. Collins, Phys. Rev. B **56**, 5164 (1997); T. J. Lenosky, J. D. Kress, L. A. Collins, and I. Kwon, J. Quant. Spectrosc. Radiat. Transf. **58**, 743 (1997).